Inorg. Chem. **2009**, *48*, 2720−2722

From Superatomic $Au_{25}(SR)_{18}^-$ to Superatomic $M@Au_{24}(SR)_{18}^q$ Core−Shell Clusters

De-en Jiang*,† and Sheng Dai†,‡

Chemical Sciences Division and Center for Nanophase Materials Science, Oak Ridge National Laboratory, Oak Ridge, Tennessee 37831

Received December 29, 2008

$Au_{25}(SR)_{18}^-$ belongs to a new type of superatom that features an icosahedral Au_{13} core−shell structure and a protective layer of six $RS(Au\text{-}SR)_2$ motifs. This superatom has a magic number of 8 free electrons that fully fill the 1s and 1p levels of the electron-shell model. By applying this superatom concept to the core-substitution chemistry of $Au_{25}(SR)_{18}^-$, we first scanned the periodic table for the potential core atom M by applying a simple rule derived from the 8-electron count and then optimized the selected candidates by density functional theory calculations to create many series of $M@Au_{24}(SR)_{18}^q$ core−shell nanoclusters. We found that 16 elements from groups 1, 2, and 10−14 of the periodic table can maintain both electronic and geometric structures of the original $Au_{25}(SR)_{18}^-$ magic cluster, indicating that the electron-counting rule based on the superatom concept is powerful in predicting viable $M@Au_{24}(SR)_{18}^q$ clusters. Our work opens up a promising area for experimental exploration.

Crystallization and structure determination of $Au_{102}(SR)_{44}$[1] and $Au_{25}(SR)_{18}^-$[2] were two recent breakthroughs in nanogold research that nicely exemplify the concept of magic numbers in alkylthiolate-protected gold (Au-SR) nanoclusters. Walter et al.[3] elegantly showed that the underlying shell-closing electron count of the metallic core of the two nanoclusters dictates the stability of the cluster. By bridging this electron count for monolayer-protected gold clusters to the traditional "superatom atomic theory" of bare metal and binary clusters,[4,5] Walter et al.'s work brought a new dimension to the "superatom" concept. Also, Akola et al.[6] correctly predicted the structure of $Au_{25}(SR)_{18}^-$ and explained its exceptional stability by its 8-electron count.

One can create new chemistry by utilizing the orbital level filling of the superatom.[7] Examples have been demonstrated for Al cluster superatoms.[8] However, these studies have relied on gas-phase experiments. Because Au-SR nanoclusters are prepared from simple wet-chemistry methods and are air and thermally stable, they allow much wider chemical functionalization and enjoy much broader applications.[9] We seek to predict superatomic thiolate-protected, gold-caged core−shell nanosystems, based on superatomic Au-SR nanoclusters. Although gold-caged metal clusters have been successfully explored,[10] they are again for the gas phase and lack a protective ligand layer against ambient conditions. In this paper, we will show that the superatom concept can be successfully applied to predict many series of simplest thiolate-protected core−shell nanoclusters by core substitution of $Au_{25}(SR)_{18}^-$ (**1**; Figure 1).

The superatom theory[3] explains that **1**'s magic stability stems from the shell-closing electron count of 8, which fully fills the 1s (2e) and 1p (6e) levels of the delocalized "superatomic orbitals" of the electron-shell model.[4] Therefore, the $Au_{25}(SR_{18})^-$ superatom is analogous to the noble-gas atom, hence exceptionally stable. How was the number 8 obtained for **1**? In short, the shell-closing electron count (n^*) for any $Au_N(SR)_L^q$ cluster is:

$$n^* = N - L - q \qquad (1)$$

where q is the charge of the cluster.[3] So, $n^* = 25 - 18 - (-1)$ yields 8 for **1**. Geometrically, **1** has a core−shell structure

* To whom correspondence should be addressed. E-mail: jiangd@ornl.gov.
† Chemical Sciences Division.
‡ Center for Nanophase Materials Science.

(1) (a) Jadzinsky, P. D.; Calero, G.; Ackerson, C. J.; Bushnell, D. A.; Kornberg, R. D. *Science* **2007**, *318*, 430. (b) Whetten, R. L.; Price, R. C. *Science* **2007**, *318*, 407.
(2) (a) Heaven, M. W.; Dass, A.; White, P. S.; Holt, K. M.; Murray, R. W. *J. Am. Chem. Soc.* **2008**, *130*, 3754. (b) Zhu, M.; Aikens, C. M.; Hollander, F. J.; Schatz, G. C.; Jin, R. *J. Am. Chem. Soc.* **2008**, *130*, 5883.
(3) Walter, M.; Akola, J.; Lopez-Acevedo, O.; Jadzinsky, P. D.; Calero, G.; Ackerson, C. J.; Whetten, R. L.; Gönbeck, H.; Häkkinen, H. *Proc. Natl. Acad. Sci. U.S.A.* **2008**, *105*, 9157.
(4) de Heer, W. A. *Rev. Mod. Phys.* **1993**, *65*, 611.
(5) Kiran, B.; Jena, P.; Li, X.; Grubisic, A.; Stokes, S. T.; Gantefor, G. F.; Bowen, K. H.; Burgert, R.; Schnöckel, H. *Phys. Rev. Lett.* **2007**, *98*, 256802.
(6) Akola, J.; Walter, M.; Whetten, R. L.; Häkkinen, H.; Grönbeck, H. *J. Am. Chem. Soc.* **2008**, *130*, 3756.
(7) Ball, P. *New Sci.* **2005**, *186*, 30.
(8) (a) Bergeron, D. E.; Roach, P. J.; Castleman, A. W.; Jones, N.; Khanna, S. N. *Science* **2005**, *307*, 231. (b) Reveles, J. U.; Khanna, S. N.; Roach, P. J.; Castleman, A. W. *Proc. Natl. Acad. Sci. U.S.A.* **2006**, *103*, 18405.
(9) Daniel, M. C.; Astruc, D. *Chem. Rev.* **2004**, *104*, 293.
(10) (a) Pyykkö, P.; Runeberg, N. *Angew. Chem., Int. Ed.* **2002**, *41*, 2174. (b) Li, X.; Kiran, B.; Li, J.; Zhai, H. J.; Wang, L. S. *Angew. Chem., Int. Ed.* **2002**, *41*, 4786. (c) Gao, Y.; Bulusu, S.; Zeng, X. C. *ChemPhysChem* **2006**, *7*, 2275. (d) Wang, L. M.; Bulusu, S.; Zhai, H. J.; Zeng, X. C.; Wang, L. S. *Angew. Chem., Int. Ed.* **2007**, *46*, 2915. (e) Sun, Q.; Wang, Q.; Jena, P.; Kawazoe, Y. *ACS Nano* **2008**, *2*, 341.

10.1021/ic8024588 CCC: $40.75
Published on Web 02/23/2009

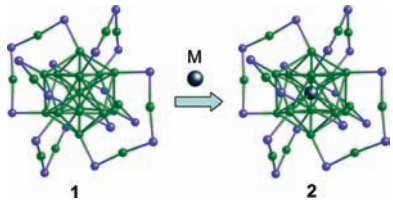

Figure 1. From **1** to M@$Au_{24}(SR)_{18}^{q}$ (**2**) by core substitution: replacing **1**'s center Au atom with a foreign atom M to create **2**, a core−shell cluster with a charge q. Color code: Au, green; S, blue; R−, not shown.

Table 1. Number of Free-Valence Electrons (x), Electron Configurations (EC), and Element Groups for the Core Atom M, for q from −2 to +2 in M@$Au_{24}(SR)_{18}^{q}$, According to Equation 2

	q				
	−2	−1	0	+1	+2
x	0	1	2	3	4
EC	$d^{10}s^0$	$d^{10}s^1$, s^1	$d^{10}s^2$, s^2	s^2p^1	s^2p^2
M	Ni, Pd, Pt	Cu, Ag, Li, Na, K, Rb, Cs	Zn, Cd, Hg, Be, Mg, Ca, Sr, Ba	B, Al, Ga, In, Tl	C, Si, Ge, Sn, Pb

of one Au atom at the center of an icosahedral Au_{12} shell[11] and an outside protective layer of six $RS(Au\text{-}SR)_2$ motifs each connecting two next-nearest-neighbor vertices of the icosahedron (Figure 1). If one substitutes the center Au atom for another element and at the same time maintains the shell-closing 8-electron count by tuning the charge q, one can create many superatom analogues of formula M@$Au_{24}(SR)_{18}^{q}$, where M is the foreign core atom. These new core−shell nanoclusters inherit from **1** a rigid geometrical shell and a protective layer, which make them suitable for wet-chemistry synthesis and applications. This idea of isoelectronic substitution, which is familiar to cluster chemists,[12] opens up the whole periodic table for consideration of M.

Suppose the core atom M has x free-valence electrons. According to eq 1, a formula M@$Au_{24}(SR)_{18}^{q}$ with $n^* = 8$ requires $x + 24 - 18 - q = 8$. Hence,

$$x = q + 2 \tag{2}$$

Equation 2 is our guiding principle for scanning the periodic table for the potential core atom. Table 1 shows five scenarios of q and corresponding x, together with their respective candidate electron configurations and groups of elements. Here we exclude highly charged scenarios (namely, $q > 2$), which we plan to explore in the future. Seven groups of elements are turned up by applying eq 2, including three groups of transition metals and four groups of main-group elements and covering about one-quarter of the elements in the periodic table.[13]

To test the viability of M@$Au_{24}(SR)_{18}^{q}$ for the elements in Table 1, we performed an in silico screening by using the density functional theory (DFT) method,[14] which has proven to be quite successful in predicting and examining the structures and dynamics of Au-SR clusters.[3,6,15] We use two criteria to judge whether an M@$Au_{24}(SR)_{18}^{q}$ core−shell cluster is viable: (1) if it maintains **1**'s electronic structure: significant highest occupied molecular orbital (HOMO)−lowest unoccupied molecular orbital (LUMO) (HL) gap and 3-fold degenerate HOMOs and doubly degenerate LUMOs;[6] (2) if it retains **1**'s icosahedral core−shell geometry.

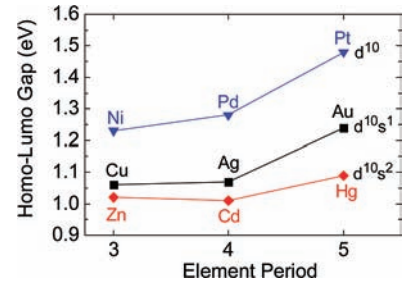

Figure 2. HOMO-LUMO gap of M@$Au_{24}(SR)_{18}^{q}$ for M being transition metals. See Table 1 for q for each group of elements.

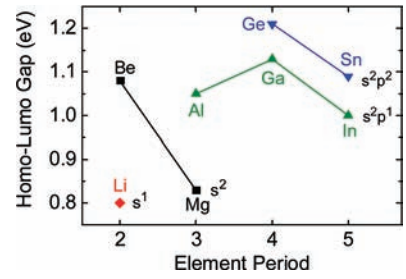

Figure 3. HOMO-LUMO gap of M@$Au_{24}(SR)_{18}^{q}$ for M being main-group elements. See Table 1 for q for each group of elements.

We optimized the structures of M@$Au_{24}(SR)_{18}^{q}$ for M in Table 1 and found that the majority of elements in Table 1 met the above two criteria except group 1 (IA) metals larger than Li, group 2 (IIA) metals larger than Mg, group 13 (IIIA) elements B and Tl, and group 14 (IVA) elements C, Si, and Pb. This DFT confirmation of the predictions of eq 2 demonstrates that the superatom concept is powerful in predicting the electronic structure of M@$Au_{24}(SR)_{18}^{q}$ nanoclusters. Figures 2 and 3 show the HL gaps for M being transition-metal and main-group elements, respectively. Below we analyze each group of M dopants.

For the same-group dopants Cu and Ag, the cluster has a HL gap ~0.2 eV lower than that of Au (1.24 eV). Zn, Cd, and Hg are stable in the center, with the cluster being neutral and the gap being between 1.0 and 1.1 eV. Placing Ni, Pd, and Pt at the cluster center requires the cluster to be a dianion. Unlike Pd, which has a d^{10} configuration, Ni and Pt have valence electron configurations of $3d^84s^2$ and $5d^96s^1$, respectively, but one can think that the two extra electrons from the charge fill up and push down their d levels, while the remaining two s electrons contribute to the superatom electron count. That is why we list Ni and Pt together with Pd under the $d^{10}s^0$ electron configuration in Table 1. We found that Pt@$Au_{24}(SR)_{18}^{2-}$ has the highest HL gap among

(11) We note that the Au_{12} shell of $Au_{25}(SR)_{18}^{-}$ is not a regular icosahedron (that is, its symmetry is lower than I_h).
(12) Mingos, D. M. P.; Wales, D. J. *Introduction to Cluster Chemistry*; Prentice-Hall: Englewood Cliffs, NJ, 1990.
(13) We did not pursue early transition metals and rare-earth elements for the center atom out of concern for their low-lying unoccupied d states interfering with the superatomic electron-shell levels.
(14) The *Turbomole V5.10* quantum chemistry program package was used. See the Supporting Information for computational details.
(15) (a) Jiang, D. E.; Tiago, M. L.; Luo, W. D.; Dai, S. *J. Am. Chem. Soc.* **2008**, *130*, 2777. (b) Pei, Y.; Gao, Y.; Zeng, X. C. *J. Am. Chem. Soc.* **2008**, *130*, 7830. (c) Jiang, D. E.; Luo, W.; Tiago, M. L.; Dai, S. *J. Phys. Chem. C* **2008**, *112*, 13905. (d) Gao, Y.; Shao, N.; Zeng, X. C. *ACS Nano* **2008**, *2*, 1497. (e) Li, Y.; Galli, G.; Gygi, F. *ACS Nano* **2008**, *2*, 1896.

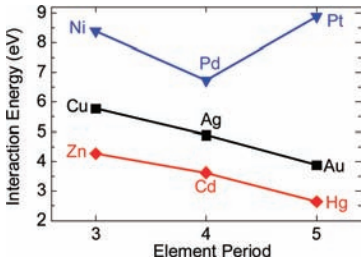

Figure 4. Interaction energy between M and the $Au_{24}(SR)_{18}^{q}$ frame for M being transition metals.

all of the elements considered, including Au itself. This indicates that Pt may be a first choice for the experimental synthesis of $M@Au_{24}(SR)_{18}^{q}$ core−shell clusters. In fact, some Pt-centered $[PtAu_x(PR_3)_y]^q$ clusters, which are isoelectronic to $[Au_{x+1}(PR_3)_y]^{q+1}$, were synthesized, for example, $[PtAu_8(PPh_3)_8]^{3+}$ and $[PtAu_{10}(PEt_3)_{10}]^{2+}$.[16] The latter cluster's Au_{10} shell can be described as an icosahedron missing two adjacent vertices.[16c] So, this cluster may be used as a precursor to make $Pt@Au_{24}(SR)_{18}^{2-}$. Encouragingly, $Au_{25}(SG)_{18}$ has been prepared by a ligand-exchange reaction of $Au_{11}(PPh_3)_8Cl_3$ with GSH (glutathione).[17]

Group 13 (IIIA) dopants except B and Tl are a good choice for the center atom. The HL gap varies between 1.0 and 1.1 eV from Al to In (Figure 3). We found that placing the B atom at the cluster center breaks the icosahedral shell because of the formation of short B−Au bonds (<2.30 Å). This is also the case for C and Si of group 14 (IVA), and only Ge and Sn of this group can maintain the geometrical and electronic structure of the $M@Au_{24}(SR)_{18}^{2+}$ superatom. Tl dramatically deforms the icosahedral shell, while Pb opens it up, probably because of their large atomic radii (1.73 and 1.75 Å, respectively, in comparison with 1.44 Å for Au).[18]

Group 1 (IA) and 2 (IIA) metals offer a quite different picture from the elements discussed above. We found that significant gaps (>0.5 eV) can be achieved only for Be, Mg, and Li. Beyond Li and Mg, both the electronic structure and the icosahedral geometry of the cluster undergo dramatic changes. For example, we found that the initial icosahedral shells of $Ca@Au_{24}(SR)_{18}$ and $Na@Au_{24}(SR)_{18}^{-}$ are broken after structural optimization. Again, we attribute this behavior to the larger atomic radii of the dopants: 1.83 Å for Na and 1.98 Å for Ca.[18] On the other hand, the $Au_{24}(SR)_{18}^{q}$ framework can accommodate Li (1.50 Å) and Mg (1.60 Å).[18]

We now examine the thermodynamic driving force for doping by computing the interaction energy[19] between the dopant and the $Au_{24}(SR)_{18}^{q}$ framework for elements in Figures 2 and 3. The results are plotted in Figures 4 and 5. One can see that for the group-to-group comparison, the

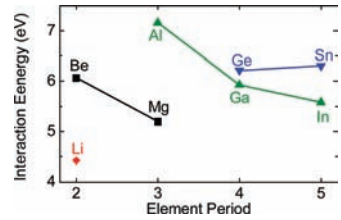

Figure 5. Interaction energy between M and the $Au_{24}(SR)_{18}^{q}$ frame for M being main-group elements.

interaction energy correlates very well the HL gap; for example, group 10 (Ni, Pd, and Pt) has the highest HL gap and also the highest interaction energy among transition metals. Within the same group, the interaction energy seems not to correlate well with the HL gap. For instance, Al has the highest interaction energy in group 13, but $Al@Au_{24}(SR)_{18}$'s HL gap is lower than $Ga@Au_{24}(SR)_{18}$'s. The fact that both the interaction energy and the HL gap depend on the optimized structure and each dopant's relaxed cluster structure is slightly different makes it difficult to correlate the HL gap to the interaction energy within the same group.

We can also relate the interaction energy between M and $Au_{24}(SR)_{18}^{q}$ to binary M−Au alloy formation. Au forms intermetallic compounds and/or solid solutions (M composition > 10 atomic %) with all of the elements in Figures 2 and 3 except Ge.[20] This fact is in line with the favorable core−frame interaction that we found for those dopants. As for Ge, our work here shows a way to achieve Ge−Au bonding though solid Ge and Au do not mix well.

In conclusion, we found that the superatom concept and its electron-count rule can be used to predict superatom analogues of $Au_{25}(SR)_{18}^{-}$ in the form of $M@Au_{24}(SR)_{18}^{q}$. To the best of our knowledge, there are no published experimental works of doping the $Au_{25}(SR)_{18}^{-}$ cluster. Therefore, our work here provides a map for such endeavors. Moreover, we expect that $M@Au_{24}(SR)_{18}^{q}$ will show interesting ligand exchange, redox chemistry, optical excitation, and luminescence properties as $Au_{25}(SR)_{18}^{-}$ does.[21] Further, our idea here can be applied to larger Au-SR nanoclusters to create larger ligand-protected core−shell nanosystems. These directions await exploration.

Acknowledgment. This work was supported by Office of Basic Energy Sciences, U.S. Department of Energy, under Contract DE-AC05-00OR22725 with UT-Battelle, LLC.

Note Added after ASAP Publication. Spelling of coauthor's name was corrected ASAP on February 25, 2009.

Supporting Information Available: Computational details, additional references, and coordinates for clusters in Figures 2 and 3. This material is available free of charge via the Internet at http://pubs.acs.org.

IC8024588

(16) (a) Mingos, D. M. P.; Watson, M. J. *Transition Met. Chem.* **1991**, *16*, 285. (b) Pignolet, L. H.; Aubart, M. A.; Craighead, K. L.; Gould, R. A. T.; Krogstad, D. A.; Wiley, J. S. *Coord. Chem. Rev.* **1995**, *143*, 219. (c) Krogstad, D. A.; Konze, W. V.; Pignolet, L. H. *Inorg. Chem.* **1996**, *35*, 6763.

(17) Shichibu, Y.; Negishi, Y.; Tsukuda, T.; Teranishi, T. *J. Am. Chem. Soc.* **2005**, *127*, 13464.

(18) Kittel, C. *Introduction to Solid State Physics*, 7th ed.; Wiley: New York, 1997.

(19) The interaction energy is defined as $E(M) + E[Au_{24}(SR)_{18}^{q}] - E[M@Au_{24}(SR)_{18}^{q}]$. The structure of the $Au_{24}(SR)_{18}^{q}$ frame is taken from the optimized $M@Au_{24}(SR)_{18}^{q}$ structure and not relaxed.

(20) Massalski, T. B. *Binary Alloy Phase Diagrams*, 2nd ed.; American Society for Metals: Metals Park, OH, 1990; Vol. 1.

(21) (a) Lee, D.; Donkers, R. L.; Wang, G. L.; Harper, A. S.; Murray, R. W. *J. Am. Chem. Soc.* **2004**, *126*, 6193. (b) Guo, R.; Murray, R. W. *J. Am. Chem. Soc.* **2005**, *127*, 12140. (c) Wang, G. L.; Huang, T.; Murray, R. W.; Menard, L.; Nuzzo, R. G. *J. Am. Chem. Soc.* **2005**, *127*, 812. (d) Wang, G. L.; Guo, R.; Kalyuzhny, G.; Choi, J. P.; Murray, R. W. *J. Phys. Chem. B* **2006**, *110*, 20282. (e) Negishi, Y.; Chaki, N. K.; Shichibu, Y.; Whetten, R. L.; Tsukuda, T. *J. Am. Chem. Soc.* **2007**, *129*, 11322. (f) Parker, J. F.; Choi, J. P.; Wang, W.; Murray, R. W. *J. Phys. Chem. C* **2008**, *112*, 13976.